Macrophage Migration Inhibitory Factor (MIF) Axis Drives Intracranial Aneurysms Macrophage M1 Polarization: Insights from Single-Cell and Bulk RNA Sequencing

Jian-huang Huang

teamhuang@sina.com

Affiliated Hospital of Putian University

Yao Chen

Affiliated Hospital of Putian University

Yuan-bao Kang

Affiliated Hospital of Putian University

Jian-ning chen

Affiliated Hospital of Putian University

Jian-hua Song

Affiliated Hospital of Putian University

Article

Keywords: single-cell sequencing, intracranial aneurysms, macrophages, vascular smooth muscle cells, macrophage migration inhibitory factor

Posted Date: April 29th, 2024

DOI: https://doi.org/10.21203/rs.3.rs-4268376/v1

Additional Declarations: No competing interests reported.

Abstract

Background: Intracranial aneurysms (IAs) develop and progress through pathological processes, including inflammation and abnormal changes in the vascular structure. The cytokine Macrophage Migration Inhibitory Factor (MIF) is implicated in the pathology of vascular diseases. However, the role of MIF in IAs remains to be elucidated.

Methods: This study utilized the Gene Expression Omnibus (GEO) database to analyze samples from IAs and normal arteries. Differential expression of MIF mRNA was assessed via Bulk-RNA sequencing (GSE54083 for testing, GSE75436 for validation), and methylation levels were examined with data from GSE75434. Single-cell transcriptomics (GSE193533) were analyzed using the Seurat package to profile Vascular smooth muscle cells (VSMCs) and macrophages. The CellChat package explored cell communication, particularly between secretory VSMCs and macrophages.

Results: Significant upregulation of MIF mRNA was observed in IAs, correlating strongly ($r=0.783$, $p=0.008$) with elevated M1-like macrophages, an indication of diagnostic potential. A corresponding decrease in MIF methylation levels and an increase in secretory VSMC proportions were noted. Elevated intercellular MIF signaling suggests it regulates VSMC-macrophage communication, influencing IAs development.

Conclusion: Our findings delineate the MIF axis as a pivotal factor in IAs pathogenesis by modulating the activity of secretory VSMCs and M1 macrophages. This axis could present novel therapeutic avenues for managing IAs, potentially stalling progression or serving as adjunctive post-surgical treatment.

Introduction

Intracranial aneurysms (IAs) represent a widespread cerebrovascular disorder, afflicting 3.2% of the population and manifesting as pathologic expansions of cerebral arteries [1]. Advances in medical imaging are increasingly bringing unruptured intracranial aneurysms (UIAs) to light, precipitating significant patient anxiety due to the dire outcomes upon rupture—a situation yielding mortality in upwards of 25% of cases [2]. Prophylactic measures for high-risk UIAs often involve invasive surgery, including aneurysm clipping or endovascular interventions, yet these carry substantial complication risks [3]. Therefore, in the face of this clinical dilemma, exploring non-invasive treatment strategies suitable for UIAs becomes particularly important.

Current research widely supports the notion that IAs are closely related to pathological processes such as inflammatory response and abnormal vascular remodeling [4]. Inflammation plays a crucial role in this process, especially the role of macrophage infiltration, which has been widely confirmed [5]. Macrophages infiltrate the arterial wall in large numbers during the formation of aneurysms [5], in stark contrast to normal cerebral arterial tissue [6]. Chronic inflammation caused by macrophages is a fundamental mechanism for the progression of IAs, continuously driving the formation and growth of aneurysms [7]. Notably, the balance between M1-like and M2-like macrophage subtypes has a significant

impact on the initiation and progression of IAs [8]. In the early stages of IAs formation, M1-like macrophage subtypes predominate, driving the formation and expansion of aneurysms by releasing pro-inflammatory factors and inducing inflammatory responses [9]. Therefore, the M1/M2 ratio in IA formation increases over time [10]. M2-like macrophages are involved in processes such as extracellular matrix clearance, vascular wall repair/remodeling, and inflammation resolution, exhibiting their unique regulatory functions [11]. At the same time, abnormal vascular remodeling is an indispensable pathological process in the formation of IAs. Under normal physiological conditions, vascular smooth muscle cells (VSMCs) respond to blood flow shear stress by synthesizing new collagen [6]. In the early stages of IAs formation, the increase in inflammatory factors is mainly concentrated in VSMCs [12], promoting the phenotypic modulation of VSMCs, i.e., the transition of VSMCs from a contractile phenotype to a secretory phenotype. This transition is marked by a reduction in the expression levels of α-smooth muscle actin (α-SMA) and smooth muscle (SM) 22α, along with an elevation in the expression of matrix metalloproteinases (MMPs). [13]. This not only weakens the strength of the vascular wall but also promotes the formation and progression of aneurysms. Although we have gained some understanding of the role of secretory VSMCs in aneurysm formation, the relationship between secretory VSMCs and macrophages remains unclear. This interaction may involve complex signaling pathways and molecular mechanisms, which are the underlying mechanisms for the formation, progression, and even rupture of IAs. Therefore, in-depth study of the interaction between secretory VSMCs and macrophages is of great significance for revealing the pathogenesis of IAs and developing new treatment strategies.

Macrophage migration inhibitory factor (MIF) is a highly conserved pleiotropic inflammatory cytokine with upstream immunomodulatory effects [14]. Given its pivotal role in vascular diseases, MIF has garnered significant attention from researchers in recent years [15, 16]. MIF secretion mainly comes from monocytes, endothelial cells, and VSMCs [17], and its expression is regulated by methylation and histone deacetylase SIRT1 [18]. Under conditions of acute stress or inflammatory stimulation, MIF is released from cells and exerts its biological functions through autocrine or paracrine mechanisms [19, 20]. MIF binds to various receptors such as CD74/CD44, CXCR4, etc., and activates downstream signaling pathways such as ERK1/2, NFκB, and AKT through phosphorylation, thereby mediating pro-inflammatory responses. This mechanism has been confirmed in various diseases such as aortic aneurysms, atherosclerosis, rheumatoid arthritis, systemic lupus erythematosus, etc. [21-25]. It is particularly worth mentioning that a Mendelian randomization study on circulating inflammatory biomarkers and the risk of IAs found that the serum MIF levels in patients with unruptured IAs were elevated [26]. In addition, recent research has reported that secretory VSMCs enhance the function of immune cells through MIF and recruit immune cell infiltration into the arterial wall, thereby promoting the growth of aortic aneurysms [25]. However, whether MIF mediates similar pathological processes in IAs is currently unclear. Considering the important role of MIF in vascular diseases and its potential connection with secretory VSMCs and macrophages, this study investigates the role of MIF in the interaction between secretory VSMCs and macrophages in IAs. This will not only help us further understand the pathogenesis of IAs, including their formation, progression, and even rupture, but may also provide important theoretical basis for the development of new treatment strategies.

Materials And Methods

Bulk-RNA Sequencing Data Source

The flow of this study is shown in Figure 1. The transcriptome data of Bulk-RNA sequencing for IAs were obtained from the Gene Expression Omnibus database (GEO) (https://www.ncbi.nlm.nih.gov/geo). The search strategy for this study included: (1) thematic search for "intracranial aneurysm"; (2) selecting "Expression profiling by array" for the Study type option; (3) samples derived from Homo sapiens; (4) datasets including normal control group samples. The mRNA sequencing of the dataset GSE54083 is based on the GPL4133 Agilent-014850 Whole Human Genome Microarray 4x44K G4112F (Feature Number version). It includes 8 ruptured intracranial aneurysm samples, 5 unruptured aneurysm samples, and 10 Superficial temporal artery samples, but ruptured intracranial aneurysm samples will be excluded in this study. The mRNA sequencing of the dataset GSE75436 is based on the GPL570 [HG-U133_Plus_2] Affymetrix Human Genome U133 Plus 2.0 Array. It contains 15 unruptured aneurysm samples and 15 Superficial temporal artery samples. In this study, dataset GSE54083 serves as the test set, and dataset GSE75436 serves as the validation set.

Differential Expression Analysis

The preliminary analysis of the Bulk-RNA sequencing dataset was based on R software (version 4.2.1; https://cran.r-project.org). Before data analysis, we performed data cleaning, including normalization and log2 processing using the "NormalizeBetweenArrays" function. Differentially expressed genes (DEGs) were identified by the "Limma" package [27]. Genes with |log2 fold change| > 0.5 and adjusted P-value < 0.05 were identified as DEGs.

Single-Cell Data Source and Data Preprocessing

Single-cell data were obtained from the GSE193533 dataset in the GEO database. This dataset involved the induction of cerebral aneurysms in adult male mice using elastase, and then single-cell RNA sequencing (scRNA-seq) was performed on the arterial samples of the Circle of Willis on the 14th day after aneurysm induction (platform: GPL30172). Our study included one intracranial aneurysm sample and one sham-treated arterial sample [28]. Using the "Seurat" R package (version 4.3.2), two Seurat objects were created separately for the intracranial aneurysm samples and sham-treated arterial samples. The "Harmony" package (version 1.2.0) was used to merge the data and remove batch effects [29]. Cells with fewer than 300 genes or mitochondrial content exceeding 10% and genes with fewer than 10 cells were removed. The count matrix was normalized and scaled using the "NormalizeData" and "ScaleData" functions in Seurat, respectively.

Cell Type Identification

Highly variable genes (HVGs) were calculated using the "FindVariableFeatures" function, and the top 20 principal components were calculated using the "RunPCA" function. Uniform Manifold Approximation and Projection (UMAP) algorithm with a resolution of 0.4 was used for cell subpopulation clustering and

visualization. To identify marker genes, we calculated DEGs through the "FindAllMarkers" function. The log fold change threshold was set at 0.5, and the significance of the differences was tested using the Wilcoxon rank-sum test. Genes with |log2 fold change| > 0.5 and adjusted P-value < 0.05 were identified as DEGs. Finally, manual cell annotation was performed using cell markers [28]. The correlation among all cell types was analyzed using Spearman's correlation analysis, and $p < 0.05$ was considered statistically significant.

Cell-to-Cell Communication Analysis

We used the "CellChat" package (version 1.6.1) to study cell-to-cell communication inferred from gene expression levels in single-cell transcriptome data. First, we conducted a holistic analysis of all cell types, inputting the gene expression profiles of all cells to identify differentially overexpressed ligands and receptors in each cell population. Interactions with p-values < 0.05 were considered statistically significant. Second, we extracted single-cell data of M1-like macrophages and secretory VSMCs to construct two separate CellChat objects and compared the differences in communication strength between different groups. Finally, significant interactions and communication strengths were visualized using circular and heatmaps.

Gene Set Enrichment Analysis

We used the "clusterProfiler" package V4.10 [30] to perform enrichment analysis of differential genes after ID conversion, including Gene Ontology biological process (GO_BP) enrichment analysis [31], Kyoto Encyclopedia of Genes and Genomes (KEGG) pathway enrichment analysis [32], and Gene Set Enrichment Analysis [33]. Terms with FDR < 0.05 were considered to be significantly enriched.

Immune Infiltration Analysis

First, the "cibersort" algorithm [34] was used to analyze the expression levels of immune cells in the test dataset for IAs and the control group. Then, we calculated the Pearson correlation coefficient and P-value between the expression of key interactome genes and immune cell expression. $P < 0.05$ was considered statistically significant and visualized using "ggplot2".

Inferred Pathway Activity

We used the "progeny" package V1.24 [35] to perform PROGENy analysis on fully annotated single-cell data. PROGENy analysis utilizes a large amount of publicly available signaling interference experiments to generate a common pathway response gene core for humans and mice, which can be used to infer pathway activity from bulk-RNA or single-cell transcriptomics.

Methylation Analysis

The methylation transcriptome data for IAs were obtained from the Gene Expression Omnibus database (GEO) (https://www.ncbi.nlm.nih.gov/geo). The search strategy for this study included: (1) thematic

search for "intracranial aneurysm"; (2) selecting "Methylation profiling by array" for the Study type option; (3) samples derived from Homo sapiens; (4) datasets including normal control group samples. The DNA methylation sequencing of the dataset GSE75434 is based on the GPL13534 Illumina HumanMethylation450 BeadChip (HumanMethylation450_15017482). It includes 9 unruptured aneurysm samples and 9 Superficial temporal artery samples.

We used the R package "ChAMP" V2.32 [36] to perform standard ChAMP procedures on the sequencing data, including data cleaning, methylation signal value matrix quality control, and differential analysis. The "PCA" function and "pheatmap" function were used to visualize the above quality control data. The expression difference analysis of methylation sites for MIF and CD74 was performed using an independent two-sample t-test, and $P < 0.05$ was considered statistically significant and visualized using "ggplot2".

Results

MIF is a Good Diagnostic Indicator for IAs and is Associated with Macrophage M1 Polarization

The mRNA sequencing data quality from dataset GSE54083 for intracranial aneurysms (IAs) and control samples was found to be satisfactory, with no significant outliers, and clear differences between the two groups (Figure 2A-C). Therefore, all samples were included in the study. Subsequently, we observed that the expression level of MIF in IAs was significantly higher than that in normal arterial samples (Figure 2D). The diagnostic ROC curve for MIF (AUC=0.980, CI=0.925-1.000) and the diagnostic PR curve, which showed a precision rate greater than 0.8, indicated its high diagnostic value for IAs (Figure 2E-F). Subsequently, we conducted an immune infiltration analysis using the Cibersort algorithm. First, the heatmap and bar chart results supported higher levels of M1-like macrophage infiltration in IAs compared to control samples (Figure 2G-H). Secondly, we found that the expression level of MIF was positively correlated with the degree of M1-like macrophage infiltration ($r=0.783$, $p=0.008$, Figure 2I). Similar results were obtained in the validation dataset GSE75436 (Supplementary Material 1). Therefore, MIF may play an important role in the pathological process of IAs and may be involved in the phenotypic polarization process of macrophages.

Levels of MIF and CD74 Methylation Are Downregulated

Upon quality assessment of the gene methylation data from both intracranial aneurysms (IAs) and normal arterial samples in the dataset GSE75434, no aberrant samples were detected. Principal Component Analysis (PCA) revealed a significant distinction between the two groupings without conspicuous correlation, thereby validating the biological grouping's relevance (Figure 3A-C). Figure 3D provides an overview of the dataset's probe detection, encompassing chromosomal loci and gene locus information. Subsequently, we conducted a differential methylation site analysis using the CHAMP pipeline. Between the two groups, there were marked differences in the methylation levels of MIF and CD74 (Figure 3E-F). As a result, the downregulation of MIF and CD74 gene methylation levels in intracranial aneurysms may contribute to the elevated mRNA expression of MIF and CD74 in IAs.

Single-Cell Data Quality Control and Cell Type Identification

After filtering out unsuitable cells and genes, a total of 9,419 cells and 17,821 genes were included. The "Harmony" package was used to integrate samples and eliminate batch effects, which demonstrated good integration (Figure 4A), with details on quality control provided in Supplementary Material 2. Setting the resolution to 0.4, an unsupervised clustering algorithm classified the 9,419 cells into 19 distinct subgroups (clusters 0-18, Figure 4B). Based on cell markers [28], manual cell annotation categorized the cells into ten defined lineages: vascular smooth muscle cells (VSMCs), endothelial cells, fibroblasts, pericytes, and immune cells (Figure 4C). The marker genes for each cell cluster are identifiable in Figure 4D. Subsequently, we examined the expression patterns of molecules related to the MIF pathway. Mif was highly expressed in VSMCs and macrophages, Pi3kr1 was moderately expressed in both VSMCs and macrophages, while Sirt1 was most abundantly expressed in VSMCs, followed by macrophages. Conversely, Nfkb1 was highly expressed in macrophages (Figure 4E). This suggests that the MIF signaling pathway may potentially mediate the interaction between VSMCs and macrophages within IAs tissue and may be particularly active.

Identification and functional analysis of VSMCs cells

We extracted the single-cell data of the VSMCs for a secondary sample integration, which showed good integration results (Figure 5A); then we performed dimensionality reduction again and clustered the 2,500 cells into 8 cell subgroups (clusters 0-7, Figure 5B). Cell identification was conducted based on the markers of VSMCs, and we discovered that the majority were secretory VSMCs (ACTA2 + MYH11 + COL1A1 + COL1A2+) followed by contractile VSMCs, while other phenotypes of VSMCs were sparse (Figures 5C-D). Subsequently, we observed a significant increase in the proportion of secretory VSMCs in IAs, while contractile VSMCs were markedly reduced (Figure 5E). Notably, there were considerable differences in the expression levels of Sirt1 and Mif among secretory VSMCs between different samples (Figure 5F). At the level of differential gene expression, secretory VSMCs expressed Tns1 and Itga9 highly and Anxa1 and S100a10 lowly (Figure 5G). Further, GO and KEGG enrichment analyses of differentially expressed genes mainly included terms like macrophage activation, positive regulation of macroautophagy, positive regulation of vascular associated smooth muscle cell migration, and the PI3K-Akt signaling pathway (Figure 5H). These findings suggest that secretory VSMCs may play an important role in the pathogenesis of IAs, especially in interaction with macrophages.

Macrophage Identification and Functional Analysis

We extracted the single-cell data of macrophages for secondary sample integration, which showed good integration results (Figure 6A); then we performed dimensionality reduction again and clustered the 2,414 cells into 10 cell subgroups (clusters 0-9, Figure 6B). Cell identification was conducted based on macrophage markers, distinguishing between M1-like and M2-like macrophages (Figure 6C). Figure 6D shows the expression level of macrophage markers in each cell subgroup. Notably, we found that the proportion of M1-like macrophages was significantly increased in the IAs tissues, and the expression levels of Pik3r1 and Nfkb1 in M1-like macrophages were also noticeably higher than in the control group

(Figures 6E-F). Subsequent differential gene expression analysis of M1-like macrophages between different samples revealed high expression of Oasl1 and Cxcl10, while Snrpf and Pim3 were expressed at low levels (Figure 6G). A global GSEA analysis indicated a strong pro-inflammatory capability of M1-like macrophages (Figure 6H), which reconfirmed the important role M1-like macrophages play in the onset and progression of IAs.

Through Spearman correlation analysis, we observed a positive correlation between secretory VSMCs and M1-like macrophages ($r=0.68$, $p<0.05$, Figure 6I). Inference of intracellular signaling pathway activity revealed significant activity of the TGFb, P53, and hypoxia pathways in secretory VSMCs, while the NFkB and TNFa signaling pathways were upregulated in M1-like macrophages (Figure 6J). This suggests that the interaction between secretory VSMCs and M1-like macrophages may be involved in the occurrence and progression of IAs.

Cell communication analysis shows a significant enhancement of the MIF axis in IAs

We conducted a comprehensive analysis of cell communication using single-cell data. First, we observed frequent cellular communication between various cell types, especially between VSMCs, fibroblasts, and macrophages (Figure 7A). Secondly, we investigated the signaling strength of different receptor-ligand interactions for MIF, where the MIF and CD74/CD44 receptor-ligand relationship dominated (Figure 7B). Chord diagrams revealed the MIF axis as an important receptor-ligand interaction between VSMCs and M1-like macrophages (Figure 7C).

Next, we extracted the single-cell data for secretory VSMCs and M1-like macrophages for group-specific cell communication analysis. First, in IAs, the interaction between secretory VSMCs and M1-like macrophages was significantly increased and enhanced compared with control group samples (Figure 7D). Secondly, through the identification of conserved and specific signaling pathways, the study further found that the signaling strength of the MIF axis between secretory VSMCs and M1-like macrophages was significantly intensified in IAs (Figure 7E). Finally, we explored the expression of the main components of the MIF axis in different cell types and found that the signaling strength of the MIF-CD74/CD44 receptor-ligand was moderate (Figures 7F-G).

Discussion

In this study, we obtained a comprehensive single-cell atlas of intracranial aneurysms (IAs) and revealed changes in the composition and functional characteristics of key cellular components in unruptured intracranial aneurysms (UIAs). We not only discovered the involvement of MIF in the pathophysiology of UIAs but also further elucidated the interactive patterns between secretory vascular smooth muscle cells (VSMCs) and M1-like macrophages, identifying the MIF-CD74 axis as a potential target for UIA. This is essential for a deeper understanding of the pathogenesis and progression of intracranial aneurysms. It is noteworthy that this study may be the first to report the contribution of the MIF-CD74 axis to UIAs.

MIF is involved in the pathophysiological processes of UIA formation and progression. Our study demonstrates that MIF mRNA expression level is significantly upregulated in UIAs, a similar phenomenon observed in aortic aneurysms [25, 37]. First, MIF is ubiquitously present and constitutively expressed in almost all mammalian cells, playing a crucial role in many physiological processes. Unlike most cytokines, MIF is constitutively synthesized and stored in intracellular pools, the release of which is triggered by pro-inflammatory and cellular stress, followed by transcription and translation of the MIF gene, replenishing the stores [19]. We also found low MIF gene methylation levels and upregulated histone deacetylase Sirt1 expression in UIAs, which may be potential mechanisms for the upregulation of MIF expression. Interestingly, both single-cell sequencing and bulk RNA sequencing from this study indicated a significant increase in MIF mRNA expression in IAs compared to normal arterial walls, suggesting the presence of an inflammatory response in the aneurysm wall, consistent with previous studies [25, 38]. Additionally, ROC and PR curves with good diagnostic performance proved MIF's involvement in the pathophysiology of UIA. Importantly, our further Cibersort algorithm infiltration analysis showed that not only was there a significant increase in the proportion of M1-like macrophages in UIAs, but the MIF expression level was positively correlated with the infiltration of M1-like macrophages, strongly indicating MIF-mediated infiltration of M1-like macrophages.

Single-cell sequencing analysis technology further clarified the source and mode of action of the increase in MIF expression in UIAs. First, we found an abundance of MIF expression in VSMCs and macrophages in UIAs, consistent with previous studies [25]. Second, the proportion of secretory VSMCs was significantly increased in UIAs, constituting one of the main components of the upregulated MIF expression. The expression of MIF receptors, however, was uneven across various cell types. We found significant expression of the MIF receptors CD74/CD44 or CD74/CXCR4 combinations only in immune cells, with CD74 abundantly expressed in M1-like macrophages. In UIAs, the downstream molecules of MIF receptors, PI3K and NFκB, were abundantly expressed in macrophages, indicating an increase in macrophage M1 polarization consistent with the rise in the proportion of M1-like macrophages [39, 40]. Furthermore, our Pearson correlation analysis confirmed a clear correlation between secretory VSMCs and M1-like macrophages. Hence, we speculate that the MIF axis may be an important factor for secretory VSMCs to mediate macrophage M1 polarization in UIA tissue.

Bearing this in mind, we conducted a cell communication analysis between secretory VSMCs and M1-like macrophages. Firstly, the overall analysis showed active MIF signaling pathways between VSMCs and M1-like macrophages. Secondly, while MIF is also expressed in normal arterial walls, the interaction between the two is rare. Conversely, the MIF signaling pathway is very active in UIAs. M1-like macrophages' MIF receptors include CD74/CD44 and CD74/CXCR4, with the former being predominant. Unlike M1-like macrophages acting on secretory VSMCs, the MIF axis is particularly critical for secretory VSMCs acting on M1-like macrophages, as no other common or significant signaling pathways were observed in our results. It is worth noting that CD44 or CXCR4 can activate NFκB signaling, which is crucial for the formation of the M1-like macrophage phenotype [41, 42].

In this study, we discovered that in UIAs, the MIF axis mediates the role of secretory VSMCs in promoting the formation of the M1-like macrophage phenotype and identified the MIF-CD74 axis as a potential target for UIAs. This forms an important basis for understanding the development and progression of intracranial aneurysms and provides new ideas for immune therapy strategies for UIAs. It should be noted that this conclusion is based on the analysis of publicly available data from public databases and requires further validation through laboratory and clinical studies. Next, we plan to establish reliable animal models to further verify these conclusions, which will require significant time and financial resources to perfect our theory. Nevertheless, it is still an important task worth pursuing.

Conclusion

In summary, we constructed a comprehensive single-cell atlas of IAs and identified the significant role of the MIF axis, particularly its mediation of secretory VSMCs in promoting the formation of the M1-like macrophage phenotype.

Declarations

Acknowledgements

Not applicable.

Authors' contributions

Jian-huang Huang analyzed the data and wrote this manuscript. Yao Chen, Yuan-bao Kang, Jian-ning Chen and Jian-hua Song assisted in analyzing the data and revising the manuscript. Yao Chen critically read and edited the manuscript.

Availability of data and materials

The datasets analyzed in this study are available for download in the Gene Expression Omnibus (GEO).

GSE54083 dataset: https://www.ncbi.nlm.nih.gov/geo/query/acc.cgi?acc=gse54083

GSE75436 dataset: https://www.ncbi.nlm.nih.gov/geo/query/acc.cgi?acc=gse 75436

GSE193533 dataset: https://www.ncbi.nlm.nih.gov/geo/query/acc.cgi?acc= gse193533

GSE75434 dataset: https://www.ncbi.nlm.nih.gov/geo/query/acc.cgi?acc= GSE75434

Data Availability Statement:

The data that support the findings of this study are available from the corresponding author upon request.

Ethics approval and consent to participate

Not applicable.

Consent for publication

Not applicable.

Competing interests

There is no competing interest to be declared by the authors.

References

1. KIM H J, SONG H N, LEE J E, et al. How Cerebral Vessel Tortuosity Affects Development and Recurrence of Aneurysm: Outer Curvature versus Bifurcation Type [J]. Journal of stroke, 2021, 23(2): 213-22.
2. CLAASSEN J, PARK S. Spontaneous subarachnoid haemorrhage [J]. Lancet, 2022, 400(10355): 846-62.
3. PONTES F G B, DA SILVA E M, BAPTISTA-SILVA J C, et al. Treatments for unruptured intracranial aneurysms [J]. Cochrane Database Syst Rev, 2021, 5(5): Cd013312.
4. PENN D L, WITTE S R, KOMOTAR R J, et al. The role of vascular remodeling and inflammation in the pathogenesis of intracranial aneurysms [J]. J Clin Neurosci, 2014, 21(1): 28-32.
5. KOSEKI H, MIYATA H, SHIMO S, et al. Two Diverse Hemodynamic Forces, a Mechanical Stretch and a High Wall Shear Stress, Determine Intracranial Aneurysm Formation [J]. Transl Stroke Res, 2020, 11(1): 80-92.
6. FRöSEN J, CEBRAL J, ROBERTSON A M, et al. Flow-induced, inflammation-mediated arterial wall remodeling in the formation and progression of intracranial aneurysms [J]. Neurosurg Focus, 2019, 47(1): E21.
7. SUZUKI H, MIKAMI T, TAMADA T, et al. Inflammation promotes progression of thrombi in intracranial thrombotic aneurysms [J]. Neurosurg Rev, 2020, 43(6): 1565-73.
8. HASAN D, CHALOUHI N, JABBOUR P, et al. Macrophage imbalance (M1 vs. M2) and upregulation of mast cells in wall of ruptured human cerebral aneurysms: preliminary results [J]. J Neuroinflammation, 2012, 9: 222.
9. MUHAMMAD S, CHAUDHRY S R, DOBREVA G, et al. Vascular Macrophages as Therapeutic Targets to Treat Intracranial Aneurysms [J]. Front Immunol, 2021, 12: 630381.
10. NOWICKI K W, HOSAKA K, WALCH F J, et al. M1 macrophages are required for murine cerebral aneurysm formation [J]. J Neurointerv Surg, 2018, 10(1): 93-7.

11. KHASHIM Z, DAYING D, HONG D Y, et al. The Distribution and Role of M1 and M2 Macrophages in Aneurysm Healing after Platinum Coil Embolization [J]. AJNR American journal of neuroradiology, 2020, 41(9): 1657-62.
12. KOLEGA J, GAO L, MANDELBAUM M, et al. Cellular and molecular responses of the basilar terminus to hemodynamics during intracranial aneurysm initiation in a rabbit model [J]. Journal of vascular research, 2011, 48(5): 429-42.
13. LUO Y, TANG H, ZHANG Z, et al. Pharmacological inhibition of epidermal growth factor receptor attenuates intracranial aneurysm formation by modulating the phenotype of vascular smooth muscle cells [J]. CNS Neurosci Ther, 2022, 28(1): 64-76.
14. SPARKES A, DE BAETSELIER P, ROELANTS K, et al. The non-mammalian MIF superfamily [J]. Immunobiology, 2017, 222(3): 473-82.
15. SINITSKI D, KONTOS C, KRAMMER C, et al. Macrophage Migration Inhibitory Factor (MIF)-Based Therapeutic Concepts in Atherosclerosis and Inflammation [J]. Thrombosis and haemostasis, 2019, 119(4): 553-66.
16. ZERNECKE A, BERNHAGEN J, WEBER C. Macrophage migration inhibitory factor in cardiovascular disease [J]. Circulation, 2008, 117(12): 1594-602.
17. KAPURNIOTU A, GOKCE O, BERNHAGEN J. The Multitasking Potential of Alarmins and Atypical Chemokines [J]. Frontiers in medicine, 2019, 6: 3.
18. HU Y, XIA W, HOU M. Macrophage migration inhibitory factor serves a pivotal role in the regulation of radiation-induced cardiac senescencethrough rebalancing the microRNA-34a/sirtuin 1 signaling pathway [J]. Int J Mol Med, 2018, 42(5): 2849-58.
19. MERK M, BAUGH J, ZIEROW S, et al. The Golgi-associated protein p115 mediates the secretion of macrophage migration inhibitory factor [J]. J Immunol, 2009, 182(11): 6896-906.
20. GREVEN D, LENG L, BUCALA R. Autoimmune diseases: MIF as a therapeutic target [J]. Expert Opin Ther Targets, 2010, 14(3): 253-64.
21. WIRTZ T H, TILLMANN S, STRüßMANN T, et al. Platelet-derived MIF: a novel platelet chemokine with distinct recruitment properties [J]. Atherosclerosis, 2015, 239(1): 1-10.
22. KONG Y Z, CHEN Q, LAN H Y. Macrophage Migration Inhibitory Factor (MIF) as a Stress Molecule in Renal Inflammation [J]. Int J Mol Sci, 2022, 23(9).
23. JANKAUSKAS S S, WONG D W L, BUCALA R, et al. Evolving complexity of MIF signaling [J]. Cell Signal, 2019, 57: 76-88.
24. BILSBORROW J B, DOHERTY E, TILSTAM P V, et al. Macrophage migration inhibitory factor (MIF) as a therapeutic target for rheumatoid arthritis and systemic lupus erythematosus [J]. Expert Opin Ther Targets, 2019, 23(9): 733-44.
25. CAO G, LU Z, GU R, et al. Deciphering the Intercellular Communication Between Immune Cells and Altered Vascular Smooth Muscle Cell Phenotypes in Aortic Aneurysm From Single-Cell Transcriptome Data [J]. Front Cardiovasc Med, 2022, 9: 936287.

26. FANG J, CAO Y, NI J. Circulating inflammatory biomarkers and risk of intracranial aneurysm: a Mendelian randomization study [J]. European journal of medical research, 2024, 29(1): 17.
27. RITCHIE M E, PHIPSON B, WU D, et al. limma powers differential expression analyses for RNA-sequencing and microarray studies [J]. Nucleic Acids Res, 2015, 43(7): e47.
28. MARTINEZ A N, TORTELOTE G G, PASCALE C L, et al. Single-Cell Transcriptome Analysis of the Circle of Willis in a Mouse Cerebral Aneurysm Model [J]. Stroke, 2022, 53(8): 2647-57.
29. KORSUNSKY I, MILLARD N, FAN J, et al. Fast, sensitive and accurate integration of single-cell data with Harmony [J]. Nat Methods, 2019, 16(12): 1289-96.
30. WU T, HU E, XU S, et al. clusterProfiler 4.0: A universal enrichment tool for interpreting omics data [J]. Innovation (Camb), 2021, 2(3): 100141.
31. ASHBURNER M, BALL C A, BLAKE J A, et al. Gene ontology: tool for the unification of biology. The Gene Ontology Consortium [J]. Nat Genet, 2000, 25(1): 25-9.
32. KANEHISA M, GOTO S. KEGG: kyoto encyclopedia of genes and genomes [J]. Nucleic Acids Res, 2000, 28(1): 27-30.
33. SUBRAMANIAN A, TAMAYO P, MOOTHA V K, et al. Gene set enrichment analysis: a knowledge-based approach for interpreting genome-wide expression profiles [J]. Proc Natl Acad Sci U S A, 2005, 102(43): 15545-50.
34. CHEN B, KHODADOUST M S, LIU C L, et al. Profiling Tumor Infiltrating Immune Cells with CIBERSORT [J]. Methods Mol Biol, 2018, 1711: 243-59.
35. SCHUBERT M, KLINGER B, KLüNEMANN M, et al. Perturbation-response genes reveal signaling footprints in cancer gene expression [J]. Nat Commun, 2018, 9(1): 20.
36. TIAN Y, MORRIS T J, WEBSTER A P, et al. ChAMP: updated methylation analysis pipeline for Illumina BeadChips [J]. Bioinformatics (Oxford, England), 2017, 33(24): 3982-4.
37. VERSCHUREN L, LINDEMAN J H, VAN BOCKEL J H, et al. Up-regulation and coexpression of MIF and matrix metalloproteinases in human abdominal aortic aneurysms [J]. Antioxidants & redox signaling, 2005, 7(9-10): 1195-202.
38. WU H, XIE C, WANG R, et al. Comparative analysis of thoracic and abdominal aortic aneurysms across the segment and species at the single-cell level [J]. Front Pharmacol, 2022, 13: 1095757.
39. LEEMANS J C, FLORQUIN S, HEIKENS M, et al. CD44 is a macrophage binding site for Mycobacterium tuberculosis that mediates macrophage recruitment and protective immunity against tuberculosis [J]. J Clin Invest, 2003, 111(5): 681-9.
40. YUNNA C, MENGRU H, LEI W, et al. Macrophage M1/M2 polarization [J]. Eur J Pharmacol, 2020, 877: 173090.
41. WANG N, LIANG H, ZEN K. Molecular mechanisms that influence the macrophage m1-m2 polarization balance [J]. Front Immunol, 2014, 5: 614.
42. DECI M B, LIU M, GONYA J, et al. Carrier-Free CXCR4-Targeted Nanoplexes Designed for Polarizing Macrophages to Suppress Tumor Growth [J]. Cellular and molecular bioengineering, 2019, 12(5):

375-88.

Figures

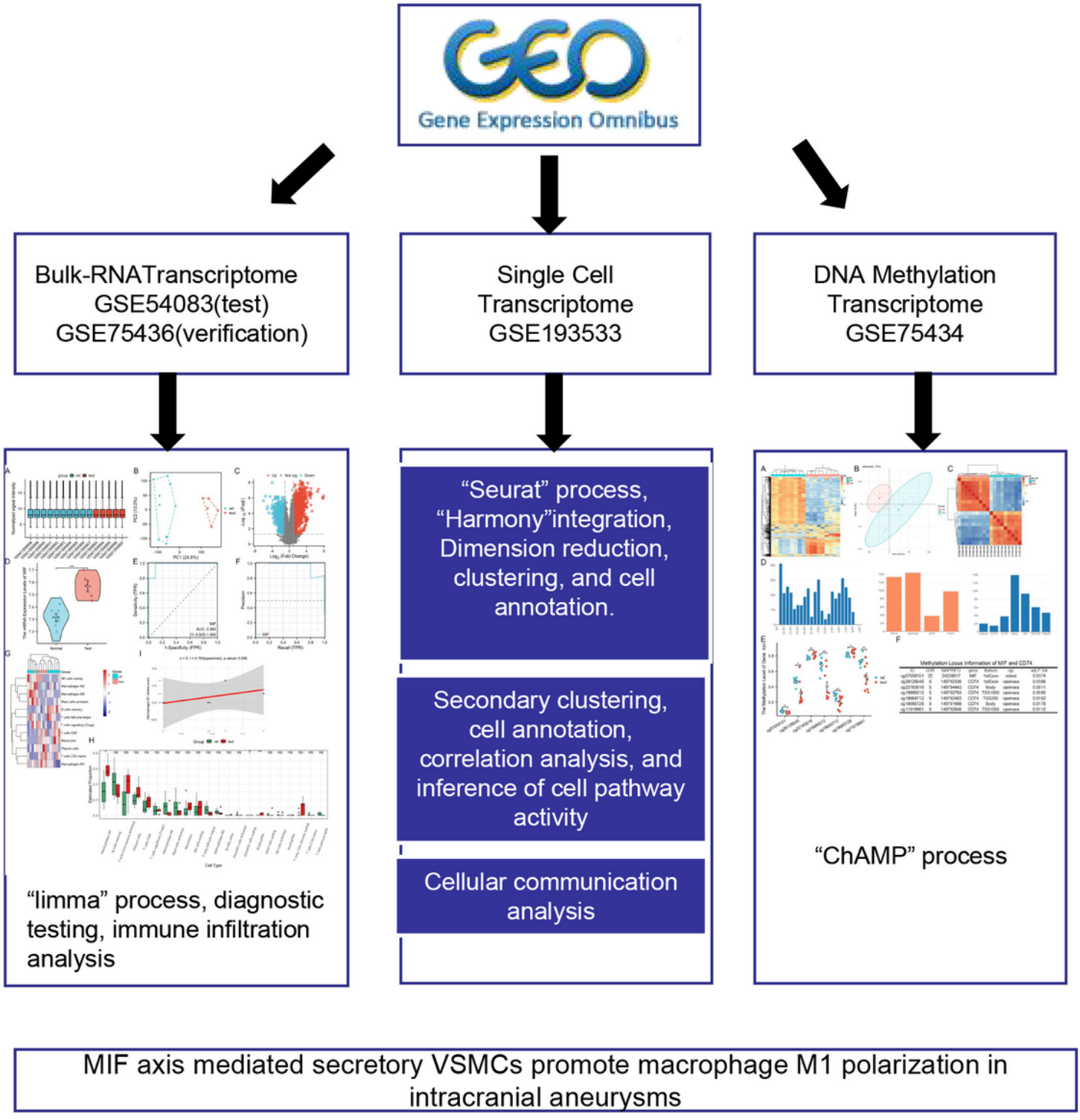

Figure 1

Flowchart of this study.

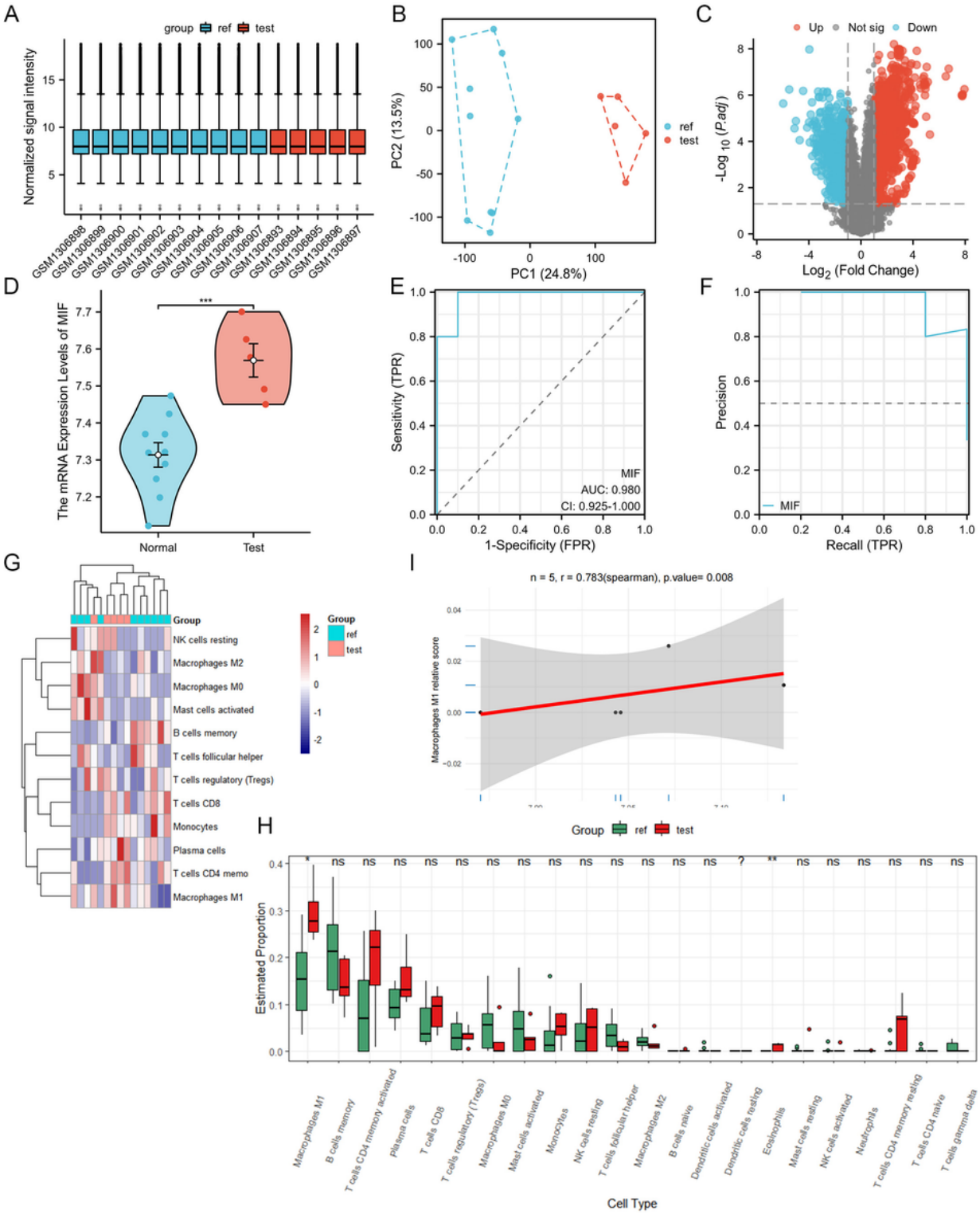

Figure 2

MIF is a Good Diagnostic Indicator for IAs and May be Associated with M1 Macrophage Polarization. A-C. The data quality control for dataset GSE54083 is satisfactory. D. The mRNA expression level of MIF in IAs is higher than in control samples. E-F. The diagnostic ROC curve and diagnostic PR curve for MIF suggest high diagnostic value for IAs. G-H. The infiltration level of M1-like macrophages in IAs is higher than in

control samples. I. There is a positive correlation between the mRNA expression level of MIF and the degree of infiltration of M1-like macrophages.

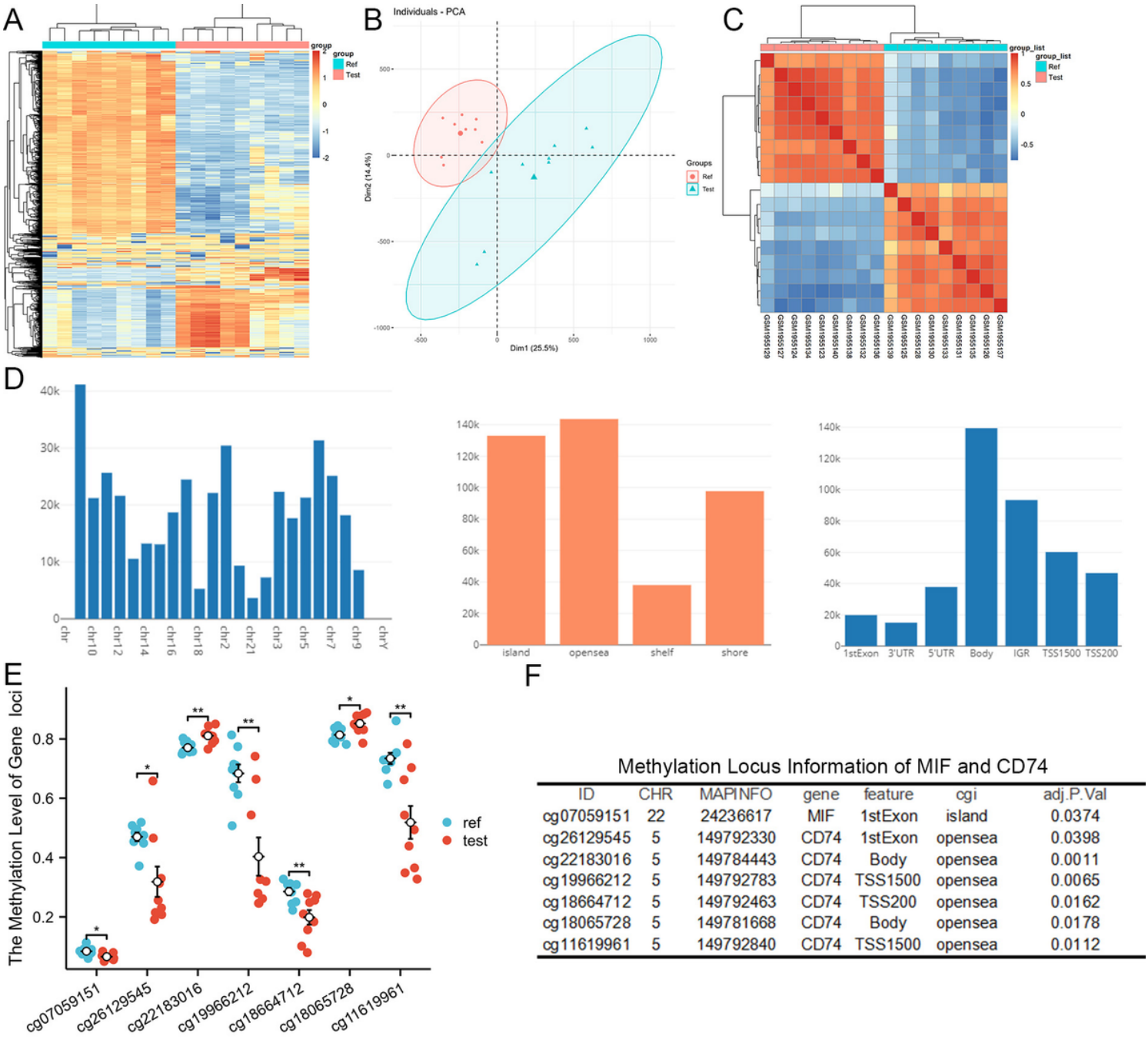

Methylation Locus Information of MIF and CD74

ID	CHR	MAPINFO	gene	feature	cgi	adj.P.Val
cg07059151	22	24236617	MIF	1stExon	island	0.0374
cg26129545	5	149792330	CD74	1stExon	opensea	0.0398
cg22183016	5	149784443	CD74	Body	opensea	0.0011
cg19966212	5	149792783	CD74	TSS1500	opensea	0.0065
cg18664712	5	149792463	CD74	TSS200	opensea	0.0162
cg18065728	5	149781668	CD74	Body	opensea	0.0178
cg11619961	5	149792840	CD74	TSS1500	opensea	0.0112

Figure 3

Methylation patterns of MIF and CD74 in dataset GSE75434. A-C. Quality control of the dataset GSE75434. D. Overview of the probe detection in dataset GSE75434. E-F. Significant differences in methylation levels of MIF and CD74 between intracranial aneurysm samples and normal cerebral arterial samples.

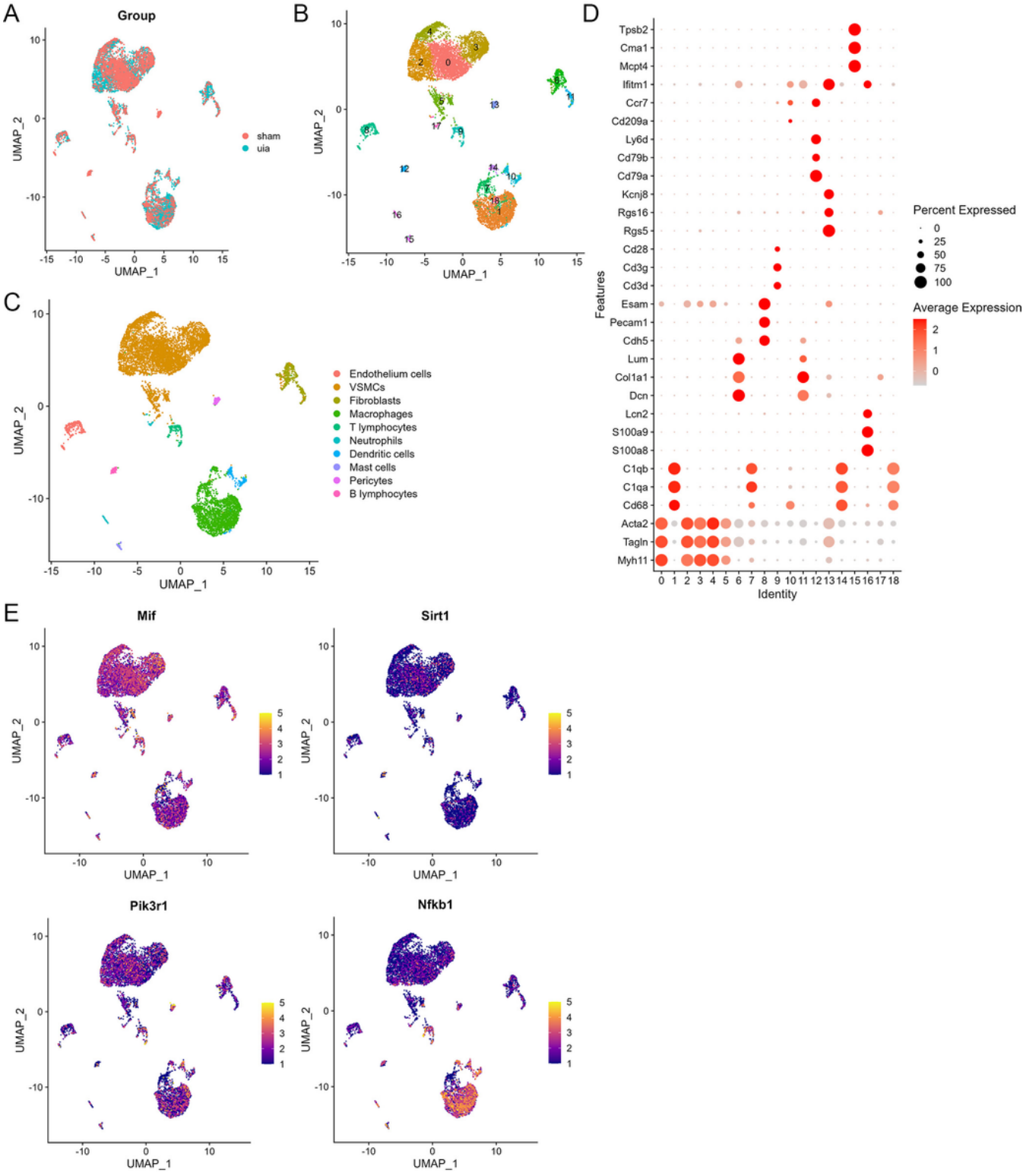

Figure 4

Single-cell atlas from dataset GSE193533. A. Single-cell data processed by the "Harmony" package showing good integration of the two groups of samples. B. 9,419 cells were dimensionality-reduced and clustered into 19 cell subgroups. C. Utilizing cell markers, 9,419 cells were annotated into 10 cell lineages. D. Expression of cell markers across all cell subgroups. E. Expression of important molecules in the MIF signaling pathway across various cell subgroups in the study data.

Identification and Functional Analysis of VSMCs

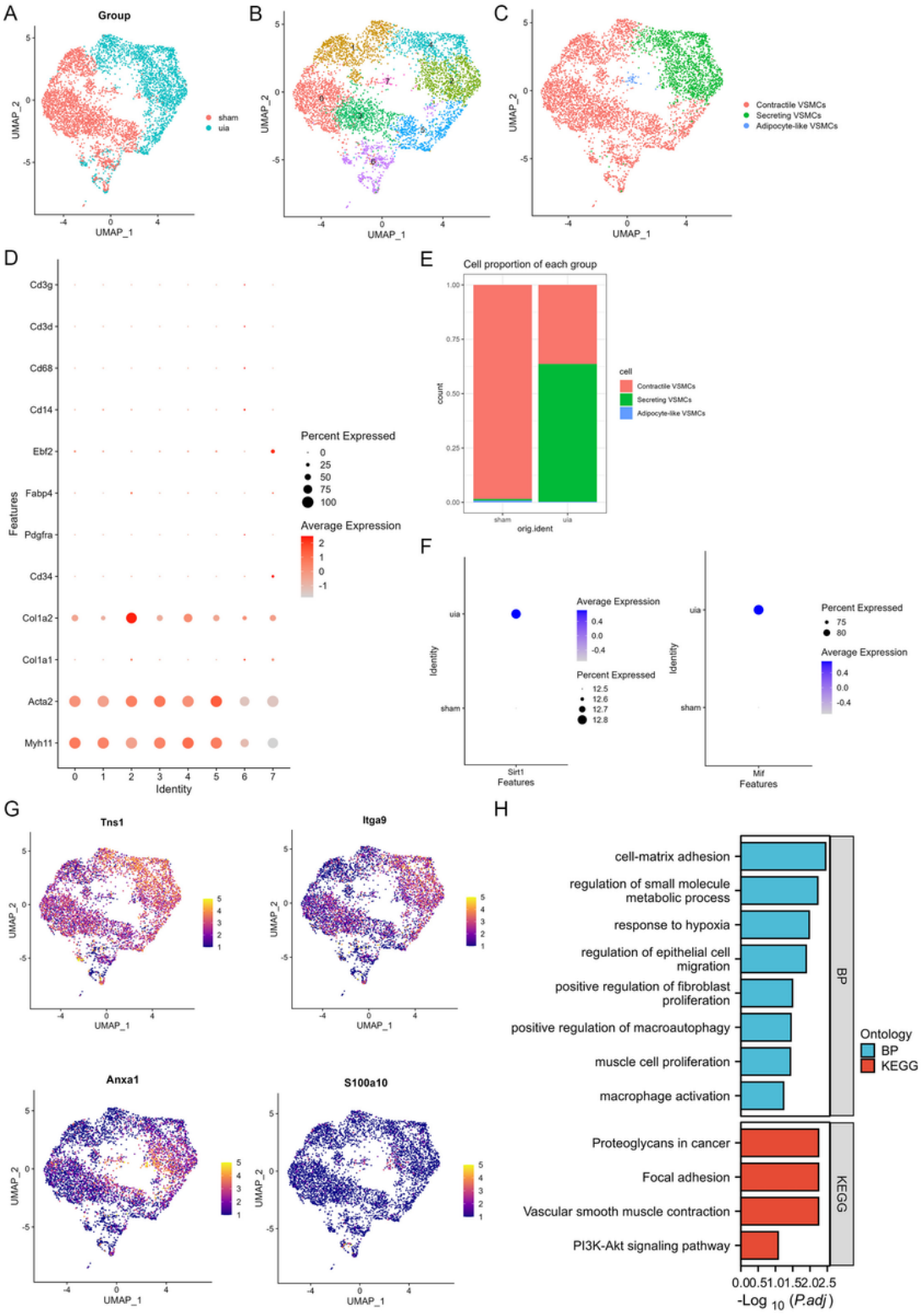

Figure 5

Single-cell atlas of vascular smooth muscle cells (VSMCs). A. Single-cell data processed by the "Harmony" package showing good integration of the two sample groups. B. UMAP plot displaying 2,500 cells dimensionality-reduced and clustered into 8 cell subgroups. C. UMAP plot showing 2,500 cells

annotated into 3 cell lineages using cell markers. D. Expression of cell markers across all cell subgroups. E. Composition of different types of VSMCs across different samples. F. Comparison of expression levels of Sirt1 and Mif in secretory VSMCs between different samples. G. UMAP plot displaying the expression of differentially expressed genes (Tns1, Itga9, Anxa1, and S100a10) in secretory VSMCs across different samples. H. Bar graph showing the results of GO and KEGG enrichment analysis for differentially expressed genes in secretory VSMCs.

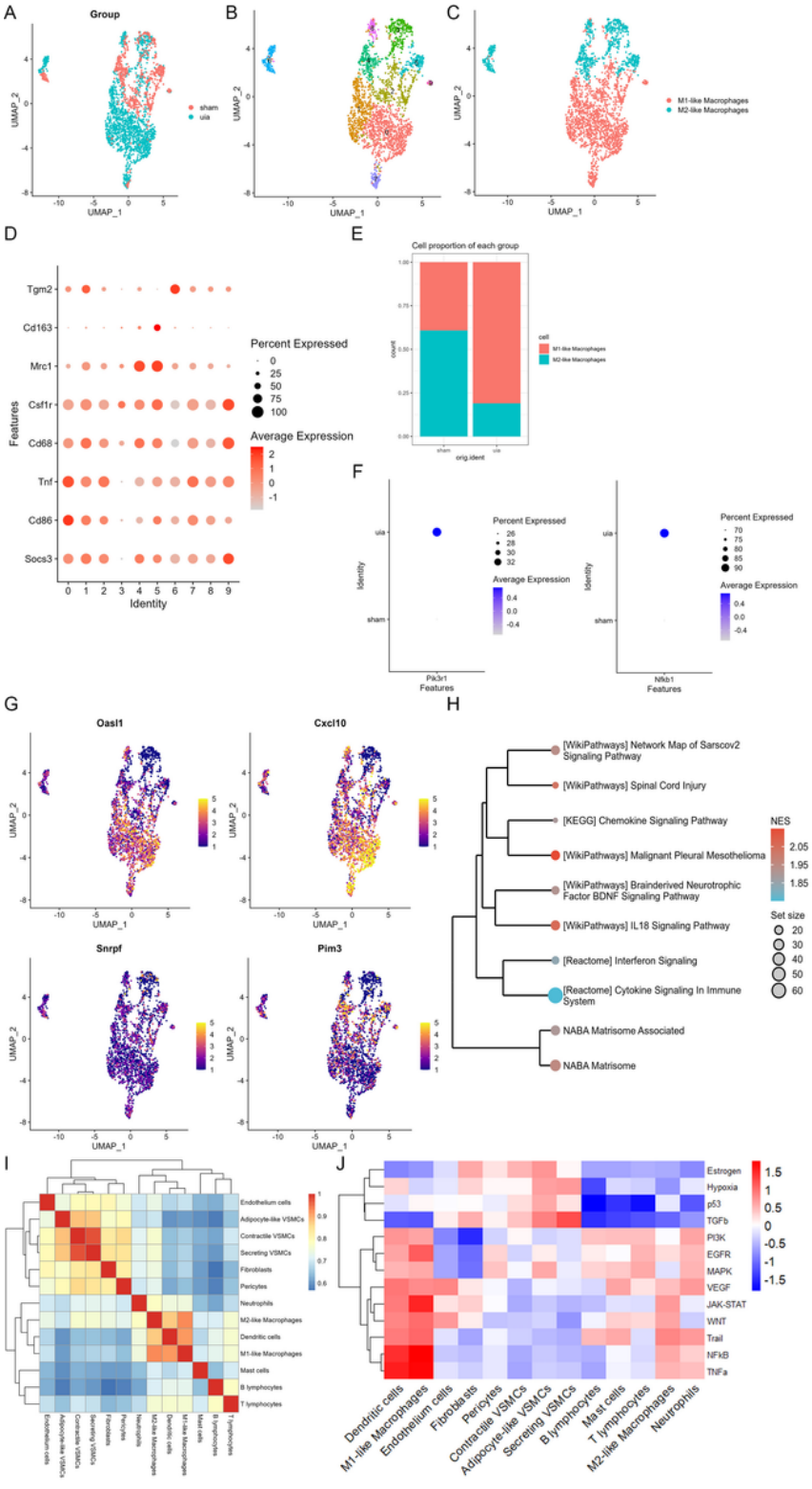

Figure 6

Macrophage identification and functional analysis. A. Single-cell data processed by the "Harmony" package show good integration of the two groups of samples. B. UMAP plot displaying 2,414 cells after dimensionality reduction and clustering into 10 cell subgroups. C. UMAP plot showing the annotation of 2,414 cells into 2 cell lineages using macrophage markers. D. Expression of macrophage markers across all cell subgroups. E. Composition of different types of macrophages across different samples. F. Comparison of expression levels of Pik3r1 and Nfkb1 in M1-like macrophages between different samples. G. UMAP plot displaying the expression of differentially expressed genes (Oasl1, Cxcl10, Snrpf, and Pim3) in M1-like macrophages across different samples. H. Dendrogram showing the GSEA enrichment analysis results for all genes in M1-like macrophages. I. Heatmap illustrating the correlation between different types of cells in dataset GSE193533. J. Heatmap showing the signal pathway activity levels of different types of cells.

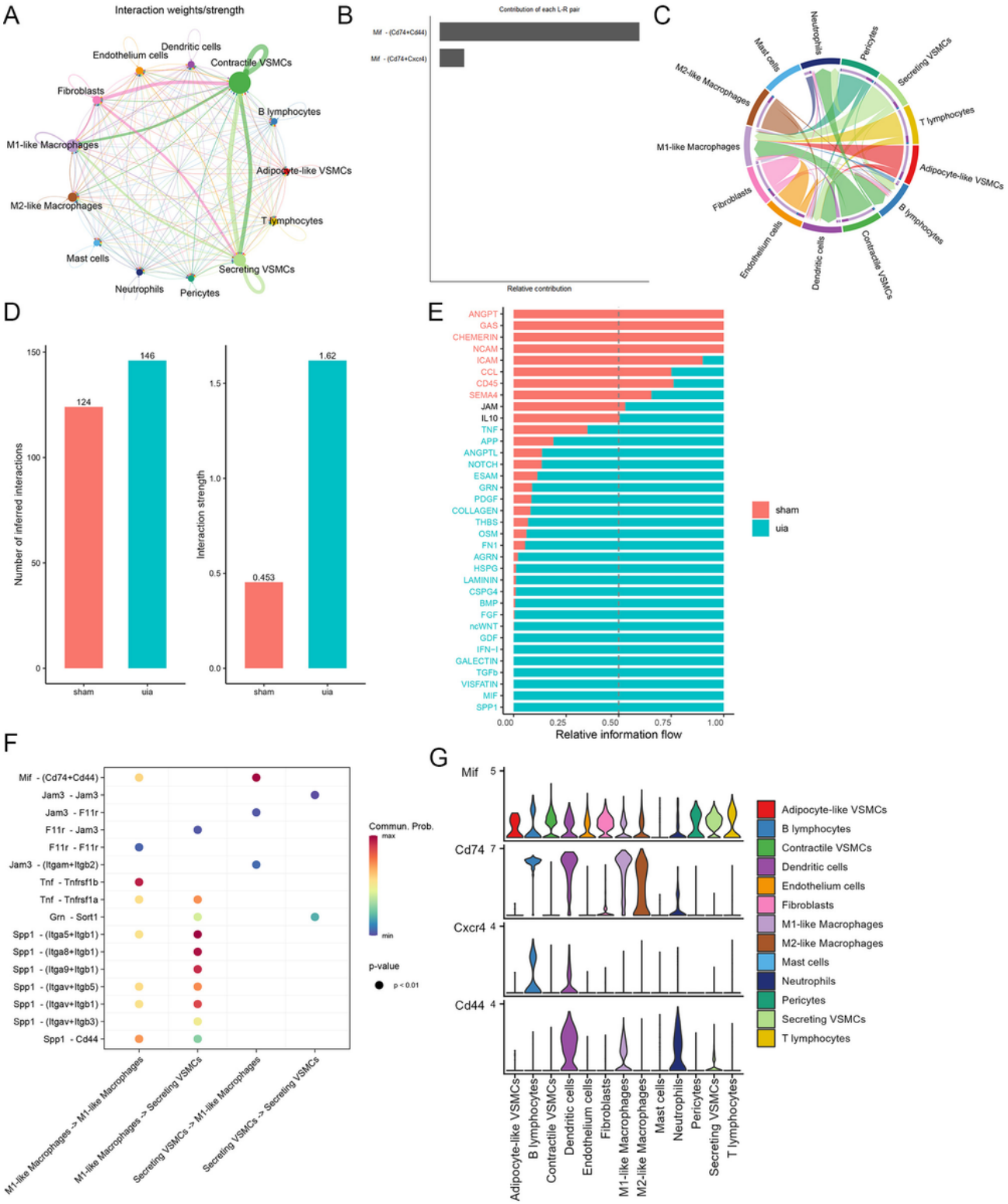

Figure 7

Results of cell communication analysis. A. Frequent cell communication exists between various cell types. B. The signaling strength of different receptor-ligand relationships in the MIF signaling pathway. C. Interaction of the MIF-CD74/CD44 signaling pathway between different cell types. D. Interaction strength and frequency between secretory VSMCs and M1-like macrophages in different groups. E. Differences in signaling pathways between secretory VSMCs and M1-like macrophages in different groups. F.

Differences in the strength of common signaling pathways between secretory VSMCs and M1-like macrophages. G. Expression of important molecules in the MIF axis across all cell types.

Supplementary Files

This is a list of supplementary files associated with this preprint. Click to download.

- SupplementaryMaterial1.doc
- SupplementaryMaterial2.doc